

ChemComm

Accepted Manuscript



This is an *Accepted Manuscript*, which has been through the Royal Society of Chemistry peer review process and has been accepted for publication.

Accepted Manuscripts are published online shortly after acceptance, before technical editing, formatting and proof reading. Using this free service, authors can make their results available to the community, in citable form, before we publish the edited article. We will replace this *Accepted Manuscript* with the edited and formatted *Advance Article* as soon as it is available.

You can find more information about *Accepted Manuscripts* in the [Information for Authors](#).

Please note that technical editing may introduce minor changes to the text and/or graphics, which may alter content. The journal's standard [Terms & Conditions](#) and the [Ethical guidelines](#) still apply. In no event shall the Royal Society of Chemistry be held responsible for any errors or omissions in this *Accepted Manuscript* or any consequences arising from the use of any information it contains.

Cite this: DOI: 10.1039/c0xx00000x

www.rsc.org/xxxxxx

ARTICLE TYPE

Hierarchical layered double hydroxide nanocomposites: structure, synthesis and applications

Zi Gu,^a John J. Atherton,^{a,b} Zhi Ping Xu,^{*a}

Received (in XXX, XXX) Xth XXXXXXXXX 20XX, Accepted Xth XXXXXXXXX 20XX

DOI: 10.1039/b000000x

Layered double hydroxide (LDH)-based nanocomposites, constructed by interacting LDH nanoparticles with other nanomaterials (e.g. silica nanoparticles and magnetic nanoparticles) or polymeric molecules (e.g. proteins), are an emerging yet active area in healthcare, environmental remediation, energy conversion and storage. Combining advantages of each component in the structure and functions, hierarchical LDH-based nanocomposites have shown great potential in biomedicine, water purification, and energy storage and conversion. This feature article summarises the recent advances in LDH-based nanocomposites, focusing on their synthesis, structure, and application in drug delivery, bio-imaging, water purification, supercapacitor, and catalysis.

1. Introduction

Recent development in material chemistry and nanotechnology has enabled scientists to develop various nanocomposites by combining different nanomaterials or modifying nanomaterials with functional molecules. The synthesised nanocomposites possess appealing and unique properties that render them attractive for application in healthcare, environmental remediation, and energy storage and conversion.¹⁻⁷

Building tailored layered double hydroxide (LDH)-based nanocomposites is an emerging area in the field of constructing 3-dimensional (3D) hierarchical nanoarchitectures with multiple functionalities. Inorganic LDH compounds, also known as hydrotalcite-like materials or anionic clays, can be found naturally as minerals and can also be readily synthesised in the laboratory.⁸ They consist of hydroxide layers of different metal cations and interlayer spacing occupied by anions and water molecules.⁸ At present, LDH nanoparticles can be tailored with the hydrodynamic diameter from 30-40 nm to 5-10 μm with various hydrothermal treatment methods.⁹⁻¹¹ In addition, through various delamination or top down methods, single-layer LDH nanosheets can be prepared, with the lateral size from 20 nm to several micrometres.¹²

Due to their rich ionic surface -OH group and the inherent positive charge, LDH nanoparticles or nanosheets can interact with other nanomaterials or polymeric molecules, generating 3D nanocomposites with particular architectures. We classify LDH-based nanocomposites into four groups, e.g. core@LDH, LDH@shell, dot-coated LDH, and targeting moiety functionalised LDH (Fig. 1). In the core-shell structure, the tailorability and functionality of LDH endow LDH with a dual role. LDH can be the shell component that is used to modify other nanoparticles including silica nanoparticles, magnesium ferrite nanoparticles, etc. (Fig. 1A), and can also be fabricated as the core coated by other nanomaterials, such as silica shell or polymeric molecule shell (Fig. 1B). The dot-coated LDH is a new

group of composites with smaller silica or metal nanoparticles being deposited on the surface of LDH (Fig. 1C). Conjugating antibody, other biopolymers or folic acid on LDH provides an opportunity for LDH targeting to the site of disease (Fig. 1D).

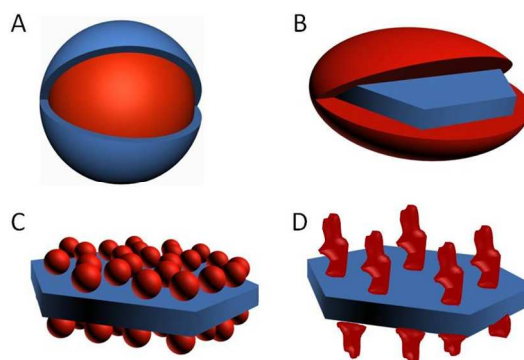


Fig. 1 Schematic illustration of LDH-based nanocomposites with different structures: (A) core@LDH (blue: LDH, red: SiO₂ nanoparticles, or magnesium ferrite nanoparticles, etc.), (B) LDH@shell (blue: LDH, red: SiO₂ nanoparticles, protein, polymer, organic hydrophobic modifier, etc.), (C) dot-coated LDH (blue: LDH, red: metal nanoparticles, SiO₂ nanoparticles, etc.), and (D) targeting moiety functionalised LDH (blue: LDH, red: folic acid, antibody, etc).

With the rapid progress of nanocomposite fabrication, the research focus has been gradually shifted to practical applications with the potential to influence our daily living conditions. The synthesised nanocomposites often possess the merits and functions of individual components, thus showing advantages over the sole nanomaterial.¹³ There are fewer published applications on environment and energy; nevertheless, the nanocomposites including silica@LDH,^{14, 15} metal oxide@LDH,¹⁶ LDH@metal,^{17, 18} LDH@polymer,¹⁹ folic acid-

conjugated LDH,²⁰ etc, have shown promise as drug delivery vectors, water pollutant removers, high-capacity supercapacitors, and cost-effective catalysts.

Tailoring the functions of LDH-related nanocomposites is a relatively new area, yet rapidly evolving area, with significant increase in the number of publications over the last 10 years (approximately 10-fold annual increase from 2004 to 2013; source from Web of Science). In 2013, Duan and co-workers published a review focusing on magnetic nanoparticle@LDH core-shell nanostructure. Until now no review paper has comprehensively summarised the basic strategies to construct 3D hierarchical LDH-based nanocomposites and their applications in the fields of biomedicine, environment remediation, and energy conversion and storage. Thus we believe that it is timely to review the latest research progress on hierarchical LDH-based nanocomposites. In this *feature article*, we summarise the recent advances in design, fabrication and potential applications of LDH-based nanocomposites with a highlight in biomedical applications, and our focus is to link a particular potential application to the hierarchical structure and building component of the corresponding nanocomposites. After a brief review of LDH nanoparticles and nanosheets in terms of concept, synthesis and applications (Section 2), the LDH-based core-shell nanoparticles are reviewed as core@LDH (Section 3) and LDH@shell (Section 4), respectively. The dot-coated LDH nanocomposites and targeting moiety-conjugated LDH nanocomposites for targeted delivery are reviewed in Section 5 and 6, respectively. In each section, we examine closely the synthesis approaches, structures, and key potential applications. In the final section (Section 7), we provide our perspective on the future developments in fabrication and application of LDH-based nanocomposites.

2. LDH nanoparticles and nanosheets

LDHs consist of brucite-like layers containing hydroxides of metal divalent and trivalent cations (M^{2+} and M^{3+} , such as Mg^{2+} , Zn^{2+} , Ni^{2+} , Al^{3+} , and Fe^{3+}). Each cation is octahedrally surrounded by six OH^- ions, and the different octahedra share edges to form a 2D layer. Between the brucite-like layers there are exchangeable anions (A^{m-} , such as CO_3^{2-} , Cl^- , and NO_3^-). The substitution of M^{2+} by M^{3+} in the hydroxide layer results in a positive charge, which is neutralised by the interlayer anion (A^{m-}). The interlayer space also contains water molecules, hydrogen bonded to layer OH^- and/or to the interlayer anions. Due to the electrostatic interactions and hydrogen bonds, the LDH forms the layered structure (Fig. 2). The general formula for these LDHs can be written as $[M^{2+}_{1-x}M^{3+}_x(OH)_2]^{x+}(A^{m-})_{x/m}\cdot nH_2O$, where $x = 0.2-0.33$, which means the M^{2+}/M^{3+} molar ratio is 2.0–4.0.^{8, 12, 21} The layer may also consist of monovalent and quadrivalent cations such as Li^+ and Ti^{4+} .⁸

Various facile synthesis methods have been studied and used to prepare LDH nanoparticles. Co-precipitation and anion exchange are the most common ones in the laboratory and conducted by simultaneously precipitating metal cations at constant or varied pH. The comprehensive study of LDH physicochemical properties and synthesis methods has led to wide applications including drug delivery carriers,²² biosensors,²³ water treatment agents,²⁴ catalysts,²⁵ supercapacitors,²⁶ etc. Due to the interlayer

anions in the LDH gallery being exchangeable, various negatively charged therapeutic molecules and pollutants in wastewaters can be intercalated into the interlayer and adsorbed on LDH surface, which could allow effective therapy and wastewater treatment, respectively.²⁷⁻²⁹ LDHs containing transition-metal elements are used as supercapacitor electrode materials, because the layered structure of LDHs provides a homogeneous dispersion of transition-metal in the matrix.³⁰

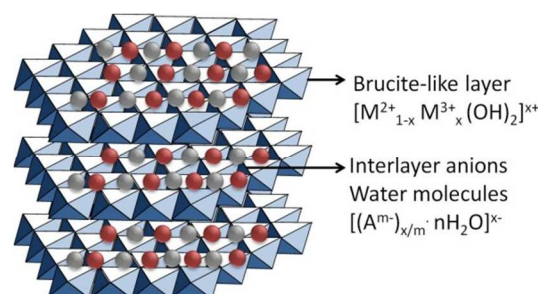


Fig. 2 Schematic illustration of layered double hydroxide structure and chemical components.

In recent years, LDH nanosheets are attracting great attention. Thanks to their 2D anisotropy with around one nanometer in thickness and tens to thousands of nanometres in lateral dimension, LDH nanosheets contribute tremendously to fundamental research and their application in building functional nanocomposites.¹² In general, LDH single sheets can be synthesised by two approaches, i.e. delamination of LDH nanoparticles and one-step synthesis of LDH monolayers.¹² Delamination of LDH nanoparticles can be achieved by using a wide variety of solvents, including butanol, acrylates, formamide, etc.;³¹⁻³³ and the one-step synthesis method employs a reverse microemulsion approach.^{34, 35} The charged nanosheets can be assembled to produce various nanoconjugates, nanofilms, and nanoarchitectures, which have tremendous potential applications in biomedicine, energy storage and energy conversion.³⁶⁻³⁸

3. Core@LDH nanocomposites

The core@LDH nanocomposites are equipped not only with the unique physicochemical properties (e.g. nanometre size and layered structure), but also with new and interesting functions (e.g. magnetism, porous structure, and high surface-to-volume ratio). We will summarise the synthesis strategy and morphology of the core@LDH nanocomposites, and their applications in drug delivery, water purification, and energy conversion and storage in this section.

3.1 Synthesis of LDH shell

The method of LDH shell synthesis is generally grouped into three categories: (1) coprecipitation; (2) sol-gel method; and (3) direct deposition (Fig. 3). Coprecipitation is a traditional and most commonly used method in the laboratory. The sol-gel method is a new and interesting approach where the linker $Al(OOH)$ serves as the substrate as well as the aluminium source. Different from the coprecipitation and sol-gel method in which LDH grows in situ on the core, direct deposition is conducted by grafting pre-synthesised LDHs on the core surface, and especially

useful to fabricate the shell consisting of LDH nanosheets.

3.1.1 Coprecipitation

Coprecipitation is a facile and commonly used method for synthesising the LDH shell. The cores that have been widely studied include silica nanospheres, metal oxide nanoparticles and nanowires, and the shells produced by coprecipitation are always LDH nanoparticles. In general, the core adsorbs two different metal cations that are subsequently precipitated on the surface of the core, and the LDH crystal growth occurs by aging at a certain temperature or through hydrothermal treatment (Fig. 3A). Zhang et al. used the coprecipitation method to prepare an anti-inflammatory drug-loaded LDH shell on the magnesium ferrite core.^{14, 39} In this work, the magnesium ferrite particle core that first adsorbed Mg^{2+} and Al^{3+} cations was mixed with a solution containing sodium hydroxide and diclofenac or ibuprofen to precipitate.^{14, 39} The synthesised magnetic drug-LDH nano hybrid possessed a clear core-shell structure with a diameter around 100 nm.^{14, 39} An earlier study by Zhang et al. reported a similar core-shell nanostructure by using the coprecipitation method.⁴⁰ However, they failed to produce homogeneous core-shell structured particles, and the particles had a network-like morphology where particle aggregation occurred. Following careful examination of the experiments in these two papers, we reasoned that ultrasonication might be a critical factor, facilitating metal cations to be evenly distributed and adsorbed on the surface of the core material and thus improving homogeneous growth of LDH. The ultrasound-assisted coprecipitation method has also been applied to synthesise a variety of core@LDH nanocomposites, such as $SiO_2@LDH$,¹⁵ $Fe_3O_4@LDH$,¹⁶ and $Y_2O_3:Er^{3+}, Yb^{3+}@SiO_2@LDH$.⁴¹

In order to fabricate the homogenous LDH nanostructure on the surface of a ferrite core, pre-coating the core by a thin layer of carbon (C-OH) or silica (SiO_2) prior to coprecipitation has been examined (Fig. 3B). A thin layer of carbon coating by the polymerisation and carbonisation of glucose through a hydrothermal reaction generates large amounts of hydrophilic groups C-OH, which facilitates the formation of the LDH shell on the ferrite core.⁴² Silica, due to its surface active -OH group, can interact effectively with metal oxide nanospheres or LDH nanoparticles to form metal oxide@ $SiO_2@LDH$ nanocomposites.³⁶ Taking advantage of this unique property of silica, Chen et al. coated $Y_2O_3:Er^{3+}, Yb^{3+}$ nanophosphors with a layer of silica and then precipitated metal cations to form LDH nanoparticles on the surface of the silica layer, and thus generated $Y_2O_3:Er^{3+}, Yb^{3+}@SiO_2@LDH$ core-shell nanoarchitecture.⁴¹

3.1.2 Sol-gel method

The first sol-gel method to fabricate LDH shells was reported by Wei and co-workers in 2010.⁴³ In this method, the boehmite ($Al(OOH)$) primer sol prepared by hydrolysing the precursor $Al(OPr)_3$ was deposited on the scaffold (i.e. paper, cloth or sponge) with several cycles of sol-gel deposition (Fig. 3C).⁴³ The generated $Al(OOH)$ coating as both substrate and source of aluminium resulted in LDH in situ growth on the scaffold (Fig. 3C).⁴³ Using this method, Shao et al. successfully synthesised $SiO_2@LDH$ and $Fe_3O_4@SiO_2@LDH$ core-shell composites with diameters of ~600 nm and ~900 nm, respectively.^{44, 45} Based on $SiO_2@LDH$ core-shell structure and the sol-gel method, the same

group also synthesised $SiO_2@LDH$ yolk-shell and hollow structure by adjusting the concentration of urea.⁴⁴ Using the sol-gel method, Wang et al. coated a much smaller SiO_2 core (50 nm, compared with Wei et al.'s 340 nm) with LDH and generated $SiO_2@LDH$ core-shell nanocomposites.⁴⁶ The sol-gel method can also be applied to grow LDH on the carbon-coated Fe_3O_4 , but failed to produce well-dispersed, homogenous core-shell particles.⁴⁷

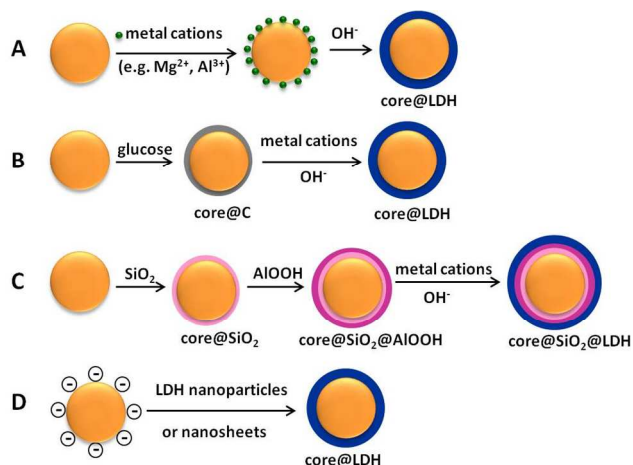


Fig. 3 Schematic illustration of the fabrication of core@LDH nanocomposites by coprecipitation (A, B), sol-gel (C), and direct deposition (D).

3.1.3 Direct deposition

In the direct deposition approach, the core material and LDH nanoparticles or nanosheets are synthesised separately, and subsequent combination of these building blocks generates a core-shell structure by self-assembling, followed by some post-treatment (Fig. 3D). Ay et al. and Li et al. used the direct deposition method to synthesise magnetic metal oxide core@LDH shell nanocomposites by adsorbing LDH nanoparticles on the core surface.^{48, 49} Li et al. also investigated the effect of post-aging temperature on the structure and physicochemical properties of the core-shell nanocomposites. With the temperature increasing from 100 to 160 °C, the LDH particles increased in size and crystallinity, and the morphology of LDH changed from flocculent-like to platelet-like shape.⁴⁹ Very interestingly, Choy and co-workers formulated Bio Core@Inorganic Shell nanohybrids with a size of around 100 nm by mixing designed DNA solution (negatively charged) and a solution containing LDH nanosheets (positively charged) together.⁵⁰ The transmission electron microscopy image of this nanocomposite showed a clear core (biomolecule, e.g. DNA)-shell (LDH) structure with the shell of ~10 nm thickness. Nonetheless, accurate control of deposited LDH density remains a challenge.

Coating LDH nanosheets on the core sphere via layer-by-layer deposition produces a multi-layered LDH shell in a controlled manner. Sasaki's group fabricated a polystyrene bead@LDH nanosheets core-shell microsphere by depositing 20 layers of poly(sodium 4-styrene sulfonate)/LDH nanosheets.^{51, 52} The core was later on used as a sacrificial template in this work. Based on

this technique, Li et al. synthesised functional $\text{Fe}_3\text{O}_4/\text{SiO}_2$ core@LDH shell nanocomposites with 20 layers of alternating carbonate and LDH nanosheets.⁵³

Electrodeposition is a widely applied coating technique in industry to graft one material on the other, and this is also useful to assemble LDH nanoparticles or nanosheets on nanowires.⁵⁴ Using this method, LDHs with positive charges are suspended in water and migrate towards the electrode scaffold (i.e. nanowire) under the influence of electrophoresis to construct 3D hierarchical metal oxide nanowire@LDH nanoarchitecture.⁵⁴

3.2 Morphology of core@LDH nanoparticles

In general, the LDH shell in the core-shell nanoarchitectures possesses three different but interactive morphologies, i.e. horizontally oriented platelet, vertically oriented platelet, and mixed platelet (Fig. 4). The horizontally oriented platelet morphology tends to be formed by direct deposition of LDH nanosheets on the core materials (described in Section 3.1.3) and possibly by coprecipitation (described in Section 3.1.1).^{50, 53} The LDH nanosheets have a high aspect ratio, large surface area, and desirable flexibility to be curved, which facilitate the nanosheets to adhere horizontally onto the sphere core. The vertically oriented platelet morphology is an interesting one that creates a porous structure, thus favoured by the researchers in the area of drug delivery and water purification. The LDH shell oriented vertically on the core is often generated by the sol-gel method (described in Section 3.1.2) and sometimes by coprecipitation.^{41, 44, 45, 55} The coexistence of horizontally and vertically oriented platelets leads to the formation of the third morphology, i.e. mixed platelet. The mixed platelet morphology was firstly denoted by Zhang et al. who fabricated magnetic core@LDH shell nanocomposites using the coprecipitation method.¹⁴ This type of morphology has been seen in most cases of coprecipitation and direct deposition,^{42, 55} and sometimes in the sol-gel method.⁴⁶

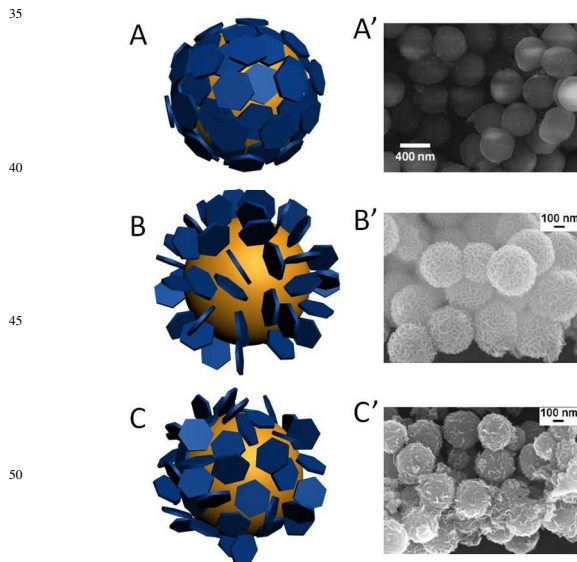


Fig. 4 Schematic illustration and SEM images of core@LDH nanoarchitectures with different morphologies: horizontally oriented platelet (A, A'), vertically oriented platelet (B, B'), and mixed platelet (C, C'). Images A'-C' are reproduced from Ref 53 and 55 with permission.

The linkage between LDH shell and metal oxide core has been proposed as MI-O-MII bonds where MI and MII represent metal cations from LDH and the core, respectively.^{40, 56} There are two possible interactions between the core and the shell via MI-O-MII bonds: (1) MI-O-MII bonds perpendicular to the LDH layer generate the horizontally oriented LDH shell, and (2) MI-O-MII bonds parallel to the LDH layer form the vertically oriented LDH shell.⁴⁰ Zhang et al. suggested that the vertically oriented LDH morphology is more easily formed because of the more unsaturated sites localised near the edge of LDH layers.⁴⁰ However, they did not give explanation on the formation of the horizontally oriented LDH shell. More recently, Chen et al. synthesised Fe_3O_4 @LDH core-shell nanocomposites with different morphologies by adjusting the methanol/water solvent ratio.⁵⁵ They found that the vertically orientated morphology was formed in the water (no methanol) environment, and the mixed morphology formed in the solvent containing methanol and water (volume ratio 1:1).⁵⁵ In their proposed mechanism, the formation of the former structure, i.e. the vertically oriented LDH, is due to the rapid nucleation of LDH compactly packed on the core surface, simultaneously upon the LDH crystal growth on the (110) plane faster than on the (003) plane.⁵⁵ Unfortunately, they did not illustrate the formation mechanism of the mixed morphology.

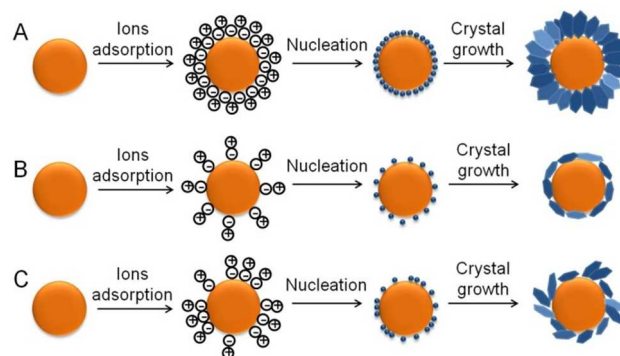


Fig. 5 Schematic illustration of formation of core@LDH nanocomposites with (A) vertically oriented, (B) horizontally oriented, and (C) mixed platelet morphology.

Here, we tentatively propose an assumption to explain the mechanism of different LDH shell morphologies formed by coprecipitation based on the formation mechanism of the vertically oriented LDH on Fe_3O_4 nanoparticle cores proposed by Chen et al.⁵⁵ When nucleation is fast, e.g. high supersaturation, the LDH nuclei are compactly packed on the core surface. Because of the limited growth space, the horizontally oriented nuclei initially formed are sacrificed and subsequently contribute to the crystal growth of the vertically oriented LDHs. Eventually, the vertically oriented LDH shell morphology becomes dominant with the growth along (110) more readily accessible than that along (003) (Fig. 5A). On the other hand, when the nucleation rate is severely restricted by some factors such as the low supersaturation or solvent, the LDH nuclei are sparsely attached on the core. As the LDH nuclei grow, the relatively smaller vertically oriented LDHs (due to the restriction of growth by the core) are sacrificed, and thus the relatively larger horizontally oriented LDH crystals become dominant (Fig. 5B). In the

situation between these two cases, the mixed platelet morphology forms (Fig. 5C). To the best of our knowledge, no one reports the horizontally oriented morphology of LDH shell formed by coprecipitation, while we still suggest the possibility to tailor the morphology of the nanocomposites by properly controlling the nucleation rate based on our assumption. Therefore, synthesis conditions that influence the nucleation rate need to be carefully examined in order to design and fabricate LDH-coated nanocomposites with a specific morphology.

3.3 Applications of core@LDH nanocomposites

Owing to their unique properties such as high surface area, magnetism and porous structure, the core@LDH nanocomposites have been examined for their application in drug delivery, water purification, and energy conversion and storage.

3.3.1 Drug delivery

Drug delivery, as one of most important applications of functional core@LDH nanocomposites, allows ideally sustained, controlled, and/or targeted delivery of therapeutic compounds with the aim of improving their therapeutic effects. The core provides a matrix for the shell growth, and more importantly endows the nanocomposite with extra functional properties, such as ferric magnetism and superparamagnetism. The LDH shell serves as an efficient drug host by intercalating/releasing the drug/gene anions into/from the LDH interlayer,^{27, 57, 58} as the interlayer anions of LDHs can be exchanged with other anions in the medium with the affinity order of $\text{CO}_3^{2-} > \text{HPO}_4^- > \text{CrO}_4^- > \text{SO}_4^{2-} > \text{OH}^- > \text{F}^- > \text{Cl}^- > \text{Br}^- > \text{NO}_3^- > \text{I}^-$.⁸ Drug/gene anions are released from the LDH shell by diffusing from the LDH interlayer and/or by LDH layer dissolution, and the drug/gene release from the composites always show a sustained release profile, in which an initial burst release can quickly establish the therapeutic dose and the subsequent prolonged release maintain this dose for a long period of time.

The drugs intercalated in the LDH shell include anti-inflammatory drugs (e.g. diclofenac, ibuprofen, and glucuronic acid),^{14, 56, 58} anti-cancer drugs (e.g. doxorubicin, doxifluridine, and 5-fluorouracil),^{41, 42, 49} and hepatitis B virus DNA vaccine.⁴⁶ Wang et al. synthesised SiO_2 @LDH nanocomposites with an average diameter of 210 nm and mixed platelet morphology.⁴⁶ They claimed that the most important advantage of this nanocomposite over other nanomaterials was its larger surface area, which could allow the loading and delivery of large amount of DNA vaccine.⁴⁶ They also found that DNA vaccine loaded- SiO_2 @LDH immunised mice demonstrated much higher serum antibody response than naked DNA vaccine, and enhanced T-cell proliferation and skewed T helper to Th1 polarisation.⁴⁶ In the physiological environment, the loaded drugs are released in a sustained manner from the nanocomposites by anion exchange and/or nanocomposite biodegradation.²⁷

Zhang et al. designed a controlled drug release device by coprecipitating the mixed platelet LDH shell with diclofenac loading on the magnesium ferrite nanoparticle core (Fig. 6A).¹⁴ Under an external magnetic field, they observed a decreased drug release rate (~20% decrease) in pH 7.45 phosphate buffer saline (PBS), which is presumably resulted from the aggregation of the magnetic nanocomposites triggered by magnetic force (Fig. 6B and 6C).^{14, 39} This group also claimed that the overall release

profile was determined by three diffusion paths of the loaded drug from the magnetic nano-hybrids (Fig. 6D): (I) intraparticle diffusion from the LDH interlayer space to the LDH interparticle space, (II) interparticle diffusion from the space among the LDH particles to the inter-aggregate space, and (III) inter-aggregate diffusion from the space among the core-shell particle aggregation to solution.¹⁴ When the magnetic field was applied, the magnetic core-shell nano-hybrids aggregated, leading to longer diffusion length, higher diffusion resistance, and a decreased drug release rate (Path III) (Fig. 6B and 6D).^{14, 39} Apart from the controlled release, targeted delivery of drugs to the diseased site using the magnetic core-shell nano-hybrids is also promising with the application of an external magnetic field.⁵⁸ Magnetic drug delivery system concentrates the drug dosage at a target site with the aid of an external magnetic field, thus avoids nonspecific drug delivery, enhances the therapeutic effect and reduces the drug side effects.^{59, 60} The targeted delivery can also be achieved by conjugating antibody and other ligands on the LDH nanoparticles,^{49, 61} and will be described in detail in Section 6.

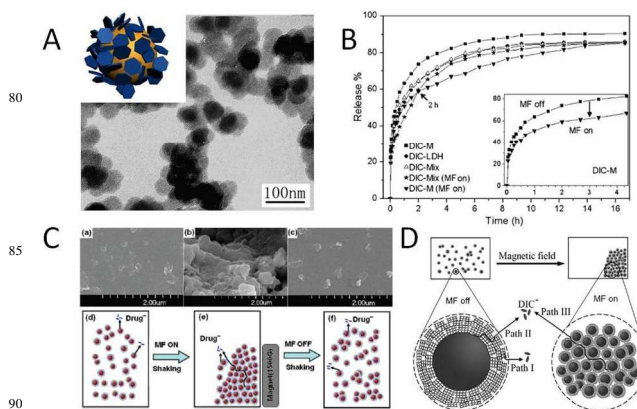


Fig. 6 (A) TEM image of diclofenac-loaded magnesium ferrite nano-hybrids (DIC-M) with the mixed platelet LDH shell. The insert shows the schematic illustration of DIC-M core@shell morphology with the mixed platelet shell. (B) Release curves of DIC from DIC-M, DIC-LDH and DIC-loaded physical mixture of magnetic nanoparticles and LDH (DIC-Mix) in pH 7.45 PBS. The insert shows the release curves of DIC-M with and without an external magnetic field. (C) SEM images and schematic illustration of the magnetic nanoparticle@LDH nano-hybrid: (a,d) without an external magnetic field, (b,e) with an external magnetic field, and (c,f) when removing the magnetic field. (D) Three diffusion paths of the loaded drugs from the magnetic nanoparticle@LDH nano-hybrid: (I) intraparticle diffusion from the LDH gallery space, (II) interparticle diffusion from the space among the LDH particles, and (III) interparticle diffusion from the space among particle aggregates to solution. Modified and reproduced from Ref 14 and 39 with permission.

3.3.2 Water purification

Pollutants in waste waters or aquatic systems have become an emerging environmental and health issue.^{62, 63} In recent years, adsorption by LDH-consisted core-shell nanoarchitecture via ion exchange is recognised as an efficient and low-cost approach to remove pollutants (i.e. acidic pharmaceutical compounds,

fluoride, and heavy metal) from waste waters.^{15, 16, 47}

Chen et al. reported a typical vertically oriented SiO₂@LDH core-shell nanocomposite synthesised by ultrasound-assisted coprecipitation (Fig. 7A), which showed much more efficient adsorption of diclofenac (a typical pharmaceutical pollutant) than LDH aggregates in terms of the adsorption rate and capacity (Fig. 7B).¹⁵ They found that the higher adsorption capacity of diclofenac on this core-shell nanocomposite (758 mg/g) than that on LDH aggregates (489 mg/g) was mainly related to the large surface area of the vertically oriented LDH shell (Fig. 7B).^{15, 64} The adsorption capacity of diclofenac by SiO₂@LDH (758 mg/g) is also obviously higher than that by polymers (324.8 mg/g)⁶⁴ and mesoporous silica (0.34 mg/g).⁶⁵ The magnetic nanoparticle@LDH core-shell nanocomposites have also been synthesised to remove fluoride ions and uranium (VI) from aqueous solutions.^{16, 47}

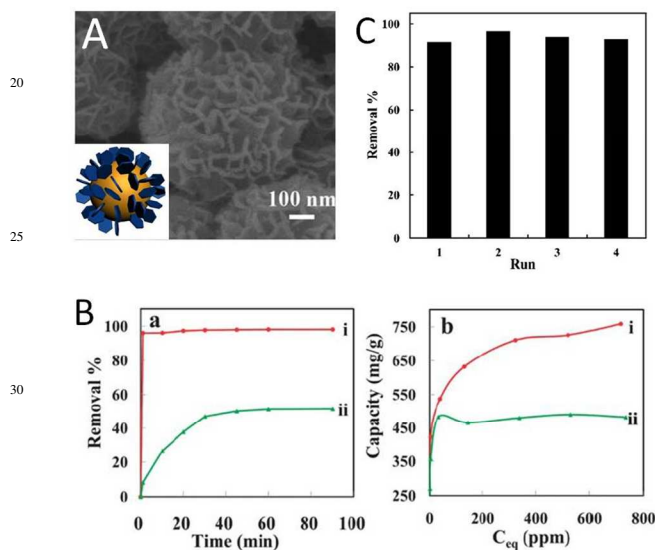


Fig. 7 (A) SEM images of SiO₂@LDH nanocomposites. The insert shows the schematic illustration of its vertically oriented platelet core-shell morphology. (B) Kinetic study (a) and adsorption isotherm (b) of diclofenac on (i) SiO₂@LDH and (ii) LDH. (C) Percentage of diclofenac removal using SiO₂@LDH in cycle runs. Modified and reproduced from Ref 15 with permission from The Royal Society of Chemistry.

After pollutant adsorption, regeneration and re-utilisation of the spent adsorbents is a vital process in large-scale cost-effective wastewater treatment. The feasible and efficient approaches to regenerating core@LDH nanohybrid adsorbents include (1) advanced oxidation to decompose the adsorbed compounds and (2) desorption of the pollutant in the eluent to re-use.^{15, 16, 47, 66} With advanced oxidation, Chen et al. reported the removal efficiency of SiO₂@LDH being consistently above 90% for at least four runs by using Co²⁺ ions and ozone as the catalyst and oxidant, respectively (Fig. 7C).¹⁵ The desorption efficiency is dependent on the affinity of intercalated anions in the LDH-based adsorbent and the anions in the eluent. In general, the eluent containing CO₃²⁻ had the highest desorption efficiency around 80%.^{16, 47}

3.3.3 Energy conversion and storage

Many efforts have been made to develop efficient and sustainable energy storage and conversion approaches because of ever worsening energy depletion and global warming.⁶⁷⁻⁶⁹ The core@LDH nanocomposites with enhanced supercapacitor and catalyst behaviour can be potentially applied in energy storage and conversion devices.⁵⁶

The characteristic properties of a supercapacitor candidate include high redox activity, high surface area, and suitable mesopore/micropore size distribution. Researchers have found that the synthesised 3D hierarchical core@LDH architectures possess these properties, and show excellent supercapacitive performance in terms of capacitance, energy density, and cycling rate.^{44, 54, 70} With different synthesis methods applied (such as deposition and sol-gel), these core@LDH architectures always have vertically orientated or mixed platelet morphology which allows the nanocomposite to form porous structure and enlarge the surface area to the maximum extent.^{44, 54, 70} The different interior hierarchy structures (SiO₂@LDH core-shell, yolk-shell, and hollow LDH shell) have also been compared in their supercapacitive performance. Shao et al. showed that the hollow NiAl-LDH structure had greatly improved faradaic redox reaction and mass transfer, and exhibited excellent pseudocapacitance performance because of the large surface area of the hollow structure, which provides effective diffusion channels for the electrolyte ions.⁴⁴ Wang et al. synthesised a hierarchical NiAl-LDH@mutiwallled carbon nanotube nanocomposite that grew on nickel foam with an exceptional areal capacitance (7.5 F/cm²) and specific capacitance (1293 F/g).⁷¹ These values are among the highest that are reported so far for other oxide/hydroxide derived architectures, such as NiTi-LDH/NF film (10.37 F/cm²),⁷² β-Ni(OH)₂/NF (2675 F/g),⁷³ hierarchical Ni_{0.25}Co_{0.75}(OH)₂ (928.4 F/g or 9.59 F/cm²)⁷⁴, hybrid nickel hydroxide/carbon nanotube (16 F/cm²),⁷⁵ and 3D nanostructure CoO@Ni(OH)₂ (11.49 F/cm²).⁷⁶ This new hierarchical structure shows as a highly promising electrode that can be applied in electrochemical energy storage.⁷¹

In addition to supercapacitor, core@LDH has been studied as a catalyst to convert acetone to diacetone alcohol as an alternative fuel component at the thermodynamic equilibrium with the conversion of 23% at 273 K.⁵⁶ The authors claimed that the catalyst was easily recovered attributed to the magnetic core and reactivity in the second run remained unchanged.⁵⁶

3.3.4 Other applications

Other applications of the core@LDH nanocomposites include immunosensor,⁶¹ DNA-based document ID system,⁵⁰ and purification of recombinant proteins.⁴⁵ Fewer studies in these interesting areas may imply that more efforts should be directed into these applications.

4. LDH@shell nanocomposites

Continuous efforts have been dedicated to producing the shell of different matters on LDH core for application in healthcare, energy conversion and storage. The functionalisation methods, including adsorption, polymerisation, etc., take advantages of LDH surface -OH groups and its surface positive charge. Thanks to the successful innovation of these methods, a variety of

functional nanomaterials (i.e. silica nanoparticles, polymers, and proteins) and small molecules (i.e. surfactant and folic acid) have been anchored on the LDH core to form various LDH@shell nanocomposites. This kind of combination can be regarded as the surface modification of LDH nanoparticles to improve LDHs' functionality, and also viewed as combining the advantages and functions of the LDHs and the functional nanomaterials for their practical applications, such as drug delivery, imaging, catalysis, and energy storage, as summarised in this section.

4.1 LDH@SiO₂

To encapsulate LDH with SiO₂ to form LDH@SiO₂ nanorattles, tetraethyl orthosilicate Si(OC₂H₅)₄ (TEOS) is used as the source of silica, and hydrolysed on the surface of LDH core (as a nuclear). The linkage between these two inorganic nanomaterials (LDH and SiO₂) is suggested to be -M-O-Si- (M is the metal cation in the brucite-like layer of LDH), as illustrated in Fig. 8.

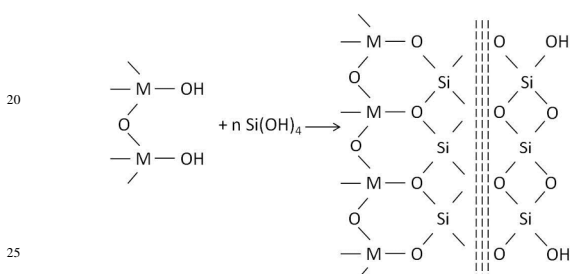


Fig. 8 Schematic illustration of the interaction between LDH and SiO₂ in LDH@SiO₂ nanostructure. M represents metal cations (e.g. Mg²⁺, Al³⁺).

In 2011, Zhao's group synthesised a novel uniform core-shell nanostructure with LDH as the core and ordered mesoporous silica as the shell.⁷⁷ The morphology of this core-shell nanocomposite observed under TEM is interesting, showing two types of nanostructures (Fig. 9A): (1) mesoporous nanoplates, and (2) rod-like cores covered by ordered mesoporous silica.⁷⁷ These two nanostructures are suggested to be projections of LDH@SiO₂ nanocomposites from two perpendicular directions (Fig. 9A).⁷⁷ By adjusting the amount of TEOS, the average thickness of the mesoporous silica shell could be tuned between 20 and 50 nm.⁷⁷ The LDH@SiO₂ nanocomposites retain the properties of both LDH and SiO₂, including high drug loading capacity, dispersivity and biocompatibility, sustained release of anionic drugs, and ready surface modification.⁷⁷ Meanwhile, Liu et al. synthesised LDH@SiO₂ nanostructure for drug delivery (Fig. 9B).⁷⁸ Although the particles were less controllable in morphology compared with Zhao group's work, they still showed sustained release of the drug and other important properties for drug delivery.⁷⁸

Apart from being a drug carrier,^{79, 80} the LDH@SiO₂ nanocomposite has been investigated as a catalyst precursor.⁸¹ Shi's group fabricated a multi-nanoparticle-embedded core@mesoporous silica shell structure.⁸¹ The core consisted of aluminium/magnesium oxides (that are then converted to LDH) and Au nanoparticles, in which the aluminium/magnesium oxides provided an essential support for Au nanoparticles, and the mesoporous silica shell offered the diffusion channels for reactants and products, allowing efficient access of reactants to

the catalytic nanoparticles inside.⁸¹

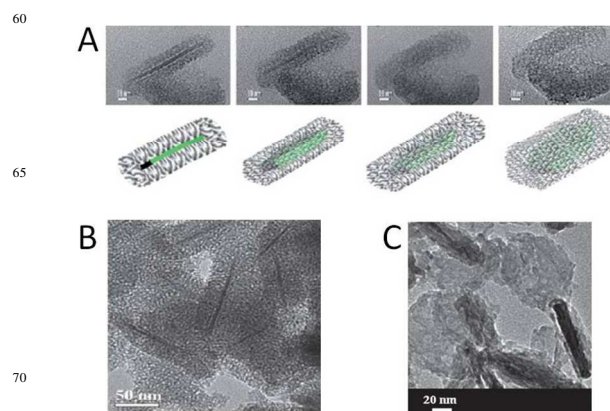


Fig. 9 TEM images of LDH@SiO₂ nanocomposites. The upper images of (A) show the TEM images of one LDH@SiO₂ nanocomposites observed at different angles by tilting the specimen with a step of 10 degrees and the bottom pictures of (A) the corresponding cartoon profile. Reproduced from Ref 77 and 78 with permission from The Royal Society of Chemistry.

4.2 LDH@protein

Protein is an amphiphilic biopolymer, and its interactions with LDH nanoparticles provide a new way to stabilise the colloidal stability, and moreover, to deliver protein/peptide-based drugs. There are a few investigations on the interactions between LDH nanoparticles and various proteins. An et al. assembled protein-adsorbed LDH nanosheets in HCl-Tris buffer, and studied the conformations and orientations of three adsorbed proteins (porcine pancreatic lipase (PPL), haemoglobin (Hb), and bovine serum albumin (BSA)) (Fig. 10).⁸² The structure and conformations of PPL were well retained because of negative charges concentrated on the side opposite to the active centres, and the orientations of PPL could be lying flat or standing up depending on the ratio of PPL and LDH (Fig. 10a). The bioactivity of PPL was thus enhanced in the hydrolysis and kinetic resolution in comparison with its soluble counterpart. The secondary structure and redox-active heme groups of Hb were not denatured either, but its tertiary or quaternary structure was changed through unfolding (Fig. 10b). The negative charges on the BSA surface were distributed along the linearly arranged domain I and II, resulting in the unfolded secondary structure (Fig. 10c). Therefore, the conformation and orientation of proteins on LDH nanosheets are dependent on the charge distribution and structural features of the proteins. These authors further suggested that the LDH nanosheet could improve the activity and stereoselectivity of at least some lipases.⁸²

Kong et al. reported the assembled LDH nanosheets with Hb and horseradish peroxidase via the layer by layer deposition technique. They found that the assembled protein/LDH electrode showed remarkable electrocatalytic activity towards oxidation of catechol in a wide linear response range, low detection limit, high stability and reproducibility.⁸³ Bellezza et al. observed that proteins (myoglobin and BSA) strongly interacted with NiAl-LDH or NiCr-LDH nanoparticles and exhibited a Langmuir-type adsorption.^{84, 85}

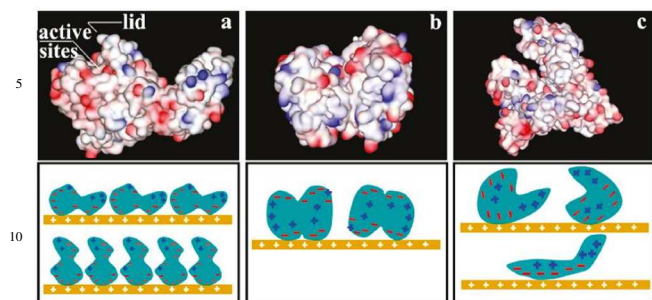


Fig. 10 Top images show electrostatic surface potentials for (a) porcine pancreatic lipase, (b) haemoglobin, (c) bovine serum albumin at pH 7.4. Bottom pictures schematically illustrate possible orientations of a) porcine pancreatic lipase, (b) haemoglobin, (c) bovine serum albumin on the positively charged 2D LDH surface. Reproduced from Ref 82 with permission.

Our group also constructed the LDH nanocomposites with ovalbumin (OVA) (Fig. 11A) and BSA coating to modulate immune response and improve LDH stability, respectively.^{86, 87} The adsorption of OVA and BSA on LDH nanoparticles was well fitted with the Langmuir model (Fig. 11B and 11C); the maximum monolayer adsorption capacity was 0.58 mg/mg for OVA (Fig. 11B),⁸⁶ and 0.70 mg/mg for BSA (Fig. 11C) on 110 nm LDH nanoparticles.⁸⁷ Coating OVA on LDH demonstrated that LDH as an adjuvant induced a high level of IgG1 antibodies comparable to Alum (an FDA approved adjuvant for human vaccination) but with much weaker inflammation.⁸⁶ BSA pre-coating prevented LDH and drug/gene-loaded LDH from aggregation in electrolyte solution (physiological environment) and enhanced the cellular uptake, possibly due to the improved colloidal stability of nanoparticles in culture medium solution.⁸⁷

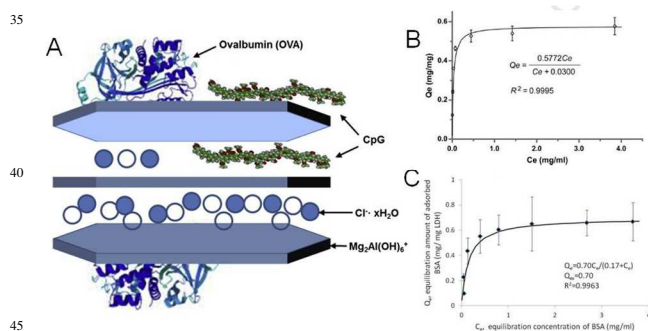


Fig. 11 (A) Schematic illustration for the Mg_2Al -LDH-based adjuvant-antigen hybrid system with OVA surface-adsorbed and CpG surface-adsorbed or intercalated. (B, C) OVA or BSA adsorption isotherm over Mg_2Al -LDH nanoparticles, and data are expressed as mean \pm SD and mean \pm SEM respectively. Reproduced from Ref 86 and 87 with permission.

4.3 LDH@polymer

There are two main methods to functionalise LDH nanoparticles with polymers: (1) adsorption of pre-synthesised polymer via electrostatic interaction,^{19, 88-90} (2) in situ polymerisation, including one-pot in situ polymerisation,⁹¹ surface-initiated atom

transfer radical polymerisation (ATPR),^{92, 93} and crosslinking.⁹⁴ Adsorption of anionic polymers on the LDH surface can be achieved by simply mixing the two components or via electrodeposition. This synthesis method takes advantages of the positive charge on the LDH surface, thus the conjugated polymers are required to be negatively charged. Because of its facile procedure, adsorption is the most common method used to synthesise LDH@polymer nanocomposites. One-pot in situ polymerisation uses LDH nanoparticles as the template/core to polymerise the anionic monomers, without washing and transferring steps. In this method, the monomer is often anchored on the LDH core via electrostatic attraction. The surface-initiated ATPR originates from the atom transfer step, which allows uniform growth of the polymeric chains.⁹⁵ Moreover, the ATPR reaction can be achieved in environmentally friendly conditions using water as the solvent.⁹⁶ Cross-linking is usually achieved by covalently cross-linking polymer that is adsorbed on the LDH surface via a cross-linked agent (e.g. glutaraldehyde).⁹⁴

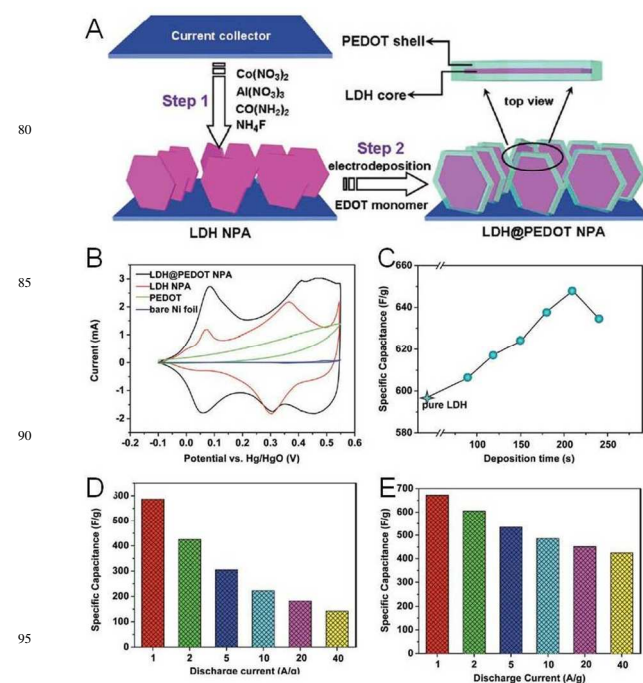


Fig. 12 (A) Schematic illustration of the fabrication of LDH@PEDOT core-shell nanoplatelet array (NPA) electrode. (B) Cyclic voltammograms of LDH NPA, PEDOT, LDH@PEDOT NPA and bare Ni foil electrode measured at a scan rate of 2 mV/s. (C) Specific capacitance of the LDH@PEDOT NPA electrode as a function of deposition time. (D, E) Specific capacitance of pristine LDH NPA and LDH@PEDOT NPA electrode respectively at various discharge current densities. Reproduced from Ref 19 with permission.

The main application of LDH@polymer nanocomposites is drug/gene delivery. Hu et al. tailored the functionality of LDH surfaces through surface-initiated ATPR of 2-(dimethylamino)-ethyl methacrylates.⁹³ This LDH composite with the flexible polycation brushes (2-(dimethylamino)-ethyl methacrylates) demonstrated increased ability to condense plasmid DNA, and

higher cellular uptake and gene transfection efficiency in COS7 and HepG2 cell lines.⁹³ Poly(ethylene glycol) (PEG) is considered a biocompatible polymer, and widely used to functionalise other drug delivery carriers with the aim of increasing colloidal stability and circulation time.⁹⁷⁻⁹⁹ For example, Li et al. synthesised anionic PEG functionalised LDH nanohybrids.⁹⁰ This LDH@PEG nanohybrid displayed enhanced colloidal stability and re-dispersing ability compared with LDH itself, due to the polymer steric hindrance and the electrostatic repulsion.⁹⁰ Colonic delivery is the other important area of LDH@polymer application. In order to improve the mucoadhesive ability and controlled release in acidic environments, the drug carrier LDH is coated with Eudragit or pectin to enhance the structural integrity in the acidic environment.^{88, 100-103}

The LDH@polymer is also applied for high-performance energy storage. Han et al. fabricated a LDH@poly(3,4-ethylenedioxythiophene) (PEDOT) core-shell nanoplatelet array (NPA) grown on a flexible Ni foil substrate as a high performance pseudocapacitor (Fig. 12A), in which LDH core provided high energy storage capacity, and the polymer shell and its porous structure facilitated electron/mass transport in the redox reaction.¹⁹ The LDH@PEDOT core-shell NPA showed a maximum specific capacitance of 649 F/g by cyclic voltammetry (scan rate was 2 mV/s) and 672 F/g by galvanostatic discharge (current density was 1 A/g) (Fig. 12B and 12C).¹⁹ The specific capacitance of the well-arranged LDH@PEDOT NPA (672 F/g) was much higher than its counterpart LDH@PEDOT-Ni foam (334 F/g), indicating that the mesoporous and well-ordered structure enhances ion diffusion of the electrolyte and electron transfer.¹⁹

4.4 LDH@organic hydrophobic modifier

Different from polymers, the organic modifiers with much smaller molecular weight are anchored on the LDH surface with the aim of modifying LDH's intrinsic hydrophilic property.

The organic modifiers include various surfactants (such as sodium dodecyl sulphate, dodecylsulfonate, and dodecylbenzenesulfonate) and other anionic organic molecules (hexanoic acid and silane coupling agent).^{89, 104-108} Hydrophobic modification of LDH is applied in drug delivery of hydrophobic pesticides and dyes,^{106, 107} as well as in biofuel production.^{105, 108} It is worth noting that some of the organic modifiers are not only anchored on the surface of LDH matrix, but also intercalated in the LDH gallery space, and the ionic affinity of the molecules may allow partial exchange of anions between LDH layers.

5. Dot-coated LDH nanocomposites

Recently, dot-coated LDH nanocomposites as a group of new hierarchical hybrid materials have attracted interest. The dot-coated LDH consists of an LDH substrate and other smaller sphere-shaped nanodots coated on the surface of LDH (Fig. 1C). Different from the LDH@shell nanocomposites, the surface of LDH is only partly covered by coated dots, thus presenting a new hierarchical structure of LDH nanocomposites and exhibiting some exciting advantages, such as the possibility of multi-functionalising LDH. Moreover, the increased particle surface roughness could also enhance cell binding and subsequent

engulfment by cells in biomedical applications.¹⁰⁹ The coating nanomaterials that have been developed include metal nanoparticles (e.g. Au nanoparticles, Pd nanoparticles, and Ag nanoparticles) and SiO₂ nanoparticles,^{17, 18, 110, 111} and the synthesised dot-coated LDHs have been examined in drug delivery and simultaneous bio-imaging, and catalysis.

5.1 Metal nanoparticles dot-coated LDH

Shi's group reported Gd-doped LDH@Au nanocomposites to dually function as a drug carrier and a diagnostic agent.¹⁸ As claimed by the authors, the advantage of this nanocomposite over other nano-systems is that the imaging agents (i.e. Gd³⁺ and Au nanoparticles) can be easily and effectively introduced into LDH and thus form the unique dot-coated nanocomposite structure. In this structure, Gd³⁺ as the magnetic resonance imaging contrast agent was doped in LDH lattice via coprecipitation method, and Au nanoparticles with an average diameter of 3.4 nm were incorporated in the nanocomposite by depositing Au(OH)₃ on the surface of LDH under alkaline condition, followed by the reduction with NaBH₄ (Fig. 13A and 13B).¹⁸ This LDH-Gd@Au nanocomposite had an average hydrodynamic diameter of around 140 nm, and was well-dispersed in water (Fig. 13C).¹⁸ By culturing mouse fibroblastic cell lines and human cervical cancer cell lines in vitro, the authors showed enhanced doxorubicin delivery efficiency with LDH-Gd@Au compared with free doxorubicin (Fig. 13D).¹⁸ Meanwhile, thanks to the component of Gd³⁺ and Au, LDH-Gd@Au nanocomposite acted efficiently as a dual-functional contrast agent for magnetic resonance imaging and X-ray computed tomography imaging in a tumour-bearing mice model (Fig. 13E).¹⁸

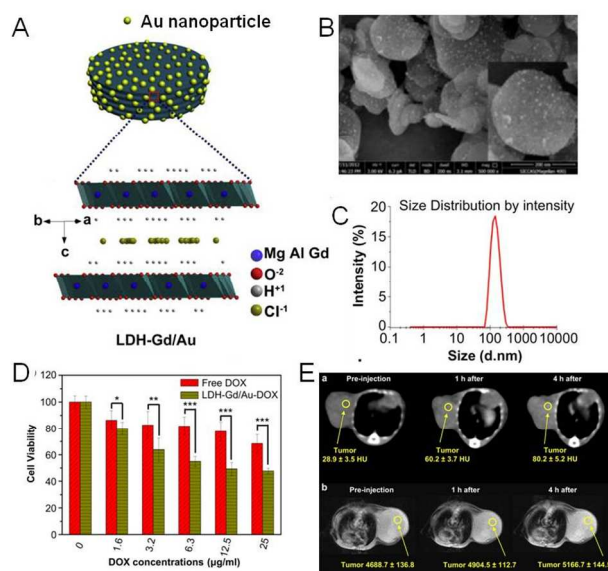


Fig. 13 (A) Schematic illustration, (B) SEM images, and (C) dynamic light scattering size distribution of LDH-Gd@Au nanocomposites. (D) HeLa cell viabilities when exposed to free doxorubicin and LDH-Gd@Au-doxorubicin at concentrations of 0-25 µg/ml (*p < 0.05, **p < 0.01, ***p < 0.001). (E) X-ray CT (upper images) and MRI (bottom images) imaging of tumour after intravenous injection of LDH-Gd@Au-heparin in 4T1 murine breast tumour-bearing mice for 0, 1, 4 h. Modified and

reproduced from Ref 18 with permission.

Zhao et al. anchored finely dispersed Pd nanodots (~1.8 nm) to CoAl-LDH nanoparticles (~1.5 μm) via a facile in situ redox reaction between the Co^{2+} in LDH nanoparticles and the PdCl_4^{2-} precursor.¹⁷ This architecture showed enhanced catalytic activity and robust durability towards ethanol electro-oxidation compared with the commercial Pd/C catalyst, in which LDH played a ternary role: catalyst support, stabiliser of Pd nanodots, and reducing agent (without any external agent).¹⁷ Zhao et al. claimed that this work provided a promising approach to fabricating highly efficient nanocatalysts that could be used in fuel cells and other related catalytic reactions.¹⁷

Apart from these two examples in biomedical and catalytic applications, metal nanoparticles, such as Ag nanoparticles and quantum dots, have also been dot-coated onto the surface of LDH and investigated in the field of sterilisation and light emitting code.^{110, 112, 113}

5.2 SiO₂ nanoparticle dot-coated LDH

Our group recently synthesised amine-functionalised SiO₂ dot-coated LDH (LDH@SiO₂-NH₂) nanocomposites via electrostatic interactions and condensation of APTES (Fig. 14a).¹¹¹ This synthesis strategy is different from the one for LDH@SiO₂ discussed in Section 4.1, with the purpose to fabricate the dot-coated nanostructure instead of the core-shell structure. SiO₂ nanodots (Z-average size of 10-15 nm, zeta potential of -38.8 mV) and LDH nanoparticles (approximately 110 nm, +42.5 mV) were synthesised separately, and then mixed to form LDH@SiO₂ nanocomposites via electrostatic attraction.¹¹¹ The nanocomposites were modified with -NH₂ by condensing APTES on the surface.¹¹¹

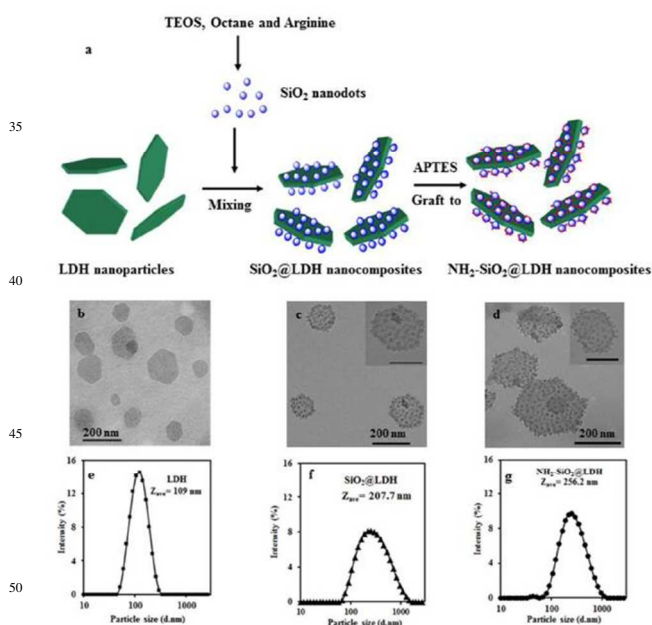


Fig. 14 (a) Schematic illustration of the synthetic process and proposed structures of functional LDH@SiO₂ nanocomposites. (b-d) TEM images of LDH (b), LDH@SiO₂ (c), and LDH@SiO₂-NH₂ (d), and the scale bars of the insert are 100 nm. (e-g) Particle size distribution of LDH (e), LDH@SiO₂ (f), and LDH@SiO₂-NH₂ (g). Reproduced from Ref 111 with permission.

The resulted LDH@SiO₂-NH₂ had the average hydrodynamic diameter of 256 nm, and showed with uniform SiO₂ nanodots of around 10-15 nm attached on the surface of LDH (Fig. 14b-14g).¹¹¹ The amine-functionalised SiO₂ dot-coating improved LDH dispersion in culture medium and PBS, and more importantly enhanced siRNA delivery to the U2OS cell line to inhibit cell proliferation, probably due to the improved nanoparticle dispersion.¹¹¹ We also suggest that the enhanced endosomal escape increases cell death,¹¹¹ in comparison with the positively charged silica nanoparticles,¹¹⁴ which seems less capable for the proton sponge effect.

6. LDH@targeting moiety

There are numerous barriers for nanoparticle-based drug carriers en route to their target, such as mucosal barriers and non-specific uptake.¹¹⁵⁻¹¹⁷ Thus it is necessary to combine the rational design of nanocarriers with moieties to encourage active targeting. This may also allow a more favourable benefit-risk profile by reducing organ toxicity, which often limits the clinical effectiveness of anthracyclines. Indeed, as tumour-free survival improves with novel chemotherapeutics, their impact of overall survival is often limited by organ toxicity, which could be potentially mitigated by nanocomposite-based drug delivery.¹¹⁸ In the case of LDH nanocarriers, recent progress in targeting moiety design has been seen in conjugating folic acid and antibody agent.^{20, 57, 119-121}

Folic acid has a high affinity (Kd \approx 100 pM) for folate receptors which are often overexpressed in various human cancers, such as ovary, lung, kidney, colon cancer, etc.¹²²⁻¹²⁵ By conjugating this cancer cell specific ligand on LDHs, Choy's group described the selectivity of this nanohybrid to folate receptor-overexpressed cell lines (i.e. human nasopharyngeal epidermoid carcinoma cells) in comparison with folate receptor deficient cell lines (i.e. human lung adenocarcinoma epithelial cells).²⁰ It is worth noting that the anionic type of folic acid can be intercalated into the LDH gallery space, which may result in the targeting function of folic acid being shielded.¹²⁶⁻¹²⁸ To address this issue, the researchers from the same group grafted folic acid on the surface of LDH by covalent coupling using silane coupling reagent APTES and 1-ethyl-3-(3-dimethylaminopropyl)-carbodiimide (EDC).²⁰ To do this, the surface of LDH nanoparticles was modified with APTES, whose amine end group could be conjugated with the functional groups such as carboxylate and thiocyanate.²⁰ For example, the activated carboxyl group of folic acid by N-hydroxysuccinimide, using EDC as coupling agents, was then combined with the amine end group of APTES on the surface of LDH to form LDH@folic acid composites.²⁰

To target vascular injury caused by surgical treatment (e.g. angioplasty), our group conjugated an anti-coagulant drug low molecular weight heparin (LMWH)-intercalated LDH nanoparticles with cross-linked fibrin antibody (an antibody that rapidly accumulates at the site of vascular injury and remains for many weeks) by associating the sulfhydryl-modified antibody with the maleimide-containing LMWH.^{121, 129-131} With this LMWH-LDH@antibody, we observed specific delivery of drugs to the site of injury, reduced luminal loss and thrombotic occlusion in a rat model of arterial injury.¹²¹

7. Conclusions and perspective

This *feature article* summarises the recent progress in synthesis approaches, physicochemical properties, and potential applications of LDH-based nanocomposites. The hierarchical LDH nanocomposites, combining the advantages of LDH nanoparticles/nanosheets and other nanomaterials/molecules, do not only show the advantages over each component of the nanocomposites, but also show some superiority to other nanomaterials such as polymers, metal oxide and mesoporous silica nanoparticles, when they are applied in drug delivery, imaging, water purification, catalysis, and energy storage. Some exciting research contributions are highlighted in this *feature article* to illustrate the unique structures, excellent properties, and important applications of the hierarchical LDH nanocomposites. In particular, the synthesis and application of dot-coated LDH nanocomposites is a new and emerging area, and worthy of further investigation, due to the virus-like surface of dot-coated LDH nanocomposites and the availability for multi-functionalisation.

Although there have been rapid advances in the synthesis and application studies of LDH-based nanocomposites, it is still a newly emerging area and there is a great deal of room for researchers to explore in this area. Constructing a new hierarchical structure will not only provide a new conceptual structure and synthesis approach, but will also offer an opportunity for potential applications. When an LDH-based nanocomposite is designed and synthesised, it is a priority question to consider whether the nanocomposite takes full use of LDH and other nanomaterials. By fabricating LDHs with different metal cations and anions, LDH could be a candidate to be used for different modes of bio-imaging as contrast agents, production of a number of compounds as a catalyst, and delivery of various therapeutic molecules.

Towards the final goal of transferring LDH-based nanocomposites from bench to industry, there are several challenges to address. One of the major challenges is to simplify the synthesis process with precise control of particle size and morphology. This is also the prerequisite for scale-up. For LDH-based nanocomposites to be used in clinics, the colloidal stability of the nanocomposites also needs to be considered, as the aggregated particles would lower the therapeutic efficacy or even block the blood vessel to cause the clot eventually. Lack of bio-safety and bio-distribution profile for healthcare application is another challenge. Future research should focus on closely linking up the nanocomposite physicochemical properties with practical applications, including, but not limited to, therapeutics, diagnosis, water and air purification, energy storage, and energy conversion.

Acknowledgements

This work was financially supported by National Health and Medical Research Council of Australia (NHMRC) Early Career Fellowship APP1073591, and Australian Research Council (ARC) Future Fellowship FT120100813.

Notes and references

- ⁵⁵ ^a Australian Institute for Bioengineering and Nanotechnology, The University of Queensland, Brisbane, QLD 4072, Australia Address, Fax: 61 07 33463973; Tel: 61 07 33463809; E-mail: z.gu@uq.edu.au (Dr. Zi Gu); gordonxu@uq.edu.au (A/Prof. Zhi Ping Xu)
- ⁵⁶ ^b Royal Brisbane and Women's Hospital, Brisbane, QLD 4006, Australia Fax: 61 07 36463257; Tel: 61 07 3646 0586; E-mail: john.atherton@health.qld.gov.au.
- † Electronic Supplementary Information (ESI) available: [details of any supplementary information available should be included here]. See DOI: 10.1039/b000000x/
1. A. Burns, H. Ow and U. Wiesner, *Chem. Soc. Rev.*, 2006, **35**, 1028-1042.
 2. R. G. Chaudhuri and S. Paria, *Chem. Rev.*, 2012, **112**, 2373-2433.
 3. G. D. Li and Z. Y. Tang, *Nanoscale*, 2014, **6**, 3995-4011.
 4. N. V. Long, Y. Yang, C. M. Thi, N. V. Minh, Y. Q. Cao and M. Nogami, *Nano Energy*, 2013, **2**, 636-676.
 5. C. Y. Li, C. Ma, F. Wang, Z. J. Xi, Z. F. Wang, Y. Deng and N. Y. He, *J. Nanosci. Nanotechnol.*, 2012, **12**, 2964-2972.
 6. S. Y. Wei, Q. Wang, J. H. Zhu, L. Y. Sun, H. F. Lin and Z. H. Guo, *Nanoscale*, 2011, **3**, 4474-4502.
 7. Y. Chen, H. R. Chen, D. P. Zeng, Y. B. Tian, F. Chen, J. W. Feng and J. L. Shi, *ACS Nano*, 2010, **4**, 6001-6013.
 8. P. S. Braterman, Z. P. Xu and F. Yarberry, *layered double hydroxides (LDHs)*, in *Handbook of Layered Materials*, eds. S. M. Auerbach, K. A. Carrado and P. K. Dutta, Marcel Dekker, New York, 2004, ch. 8, pp. 373-474.
 9. Z. P. Xu, G. S. Stevenson, C. Q. Lu, G. Q. M. Lu, P. F. Bartlett and P. P. Gray, *J. Am. Chem. Soc.*, 2006, **128**, 36-37.
 10. E. Gardner, K. M. Huntoon and T. J. Pinnavaia, *Adv. Mater.*, 2001, **13**, 1263-1266.
 11. Y. Arai and M. Ogawa, *Appl. Clay Sci.*, 2009, **42**, 601-604.
 12. Q. Wang and D. O'Hare, *Chem. Rev.*, 2012, **112**, 4124-4155.
 13. J. Liu, S. Z. Qiao, J. S. Chen, X. W. Lou, X. R. Xing and G. Q. Lu, *Chem. Commun.*, 2011, **47**, 12578-12591.
 14. H. Zhang, D. K. Pan, K. Zou, J. He and X. Duan, *J. Mater. Chem.*, 2009, **19**, 3069-3077.
 15. C. P. Chen, P. H. Wang, T. T. Lim, L. H. Liu, S. M. Liu and R. Xu, *J. Mater. Chem. A*, 2013, **1**, 3877-3880.
 16. Q. Chang, L. H. Zhu, Z. H. Luo, M. Lei, S. C. Zhang and H. Q. Tang, *Ultrason. Sonochem.*, 2011, **18**, 553-561.
 17. J. W. Zhao, M. F. Shao, D. P. Yan, S. T. Zhang, Z. Z. Lu, Z. X. Li, X. Z. Cao, B. Y. Wang, M. Wei, D. G. Evans and X. Duan, *J. Mater. Chem. A*, 2013, **1**, 5840-5846.
 18. L. J. Wang, H. Y. Xing, S. J. Zhang, Q. G. Ren, L. M. Pan, K. Zhang, W. B. Bu, X. P. Zheng, L. P. Zhou, W. J. Peng, Y. Q. Hua and J. L. Shi, *Biomaterials*, 2013, **34**, 3390-3401.
 19. J. B. Han, Y. B. Dou, J. W. Zhao, M. Wei, D. G. Evans and X. Duan, *Small*, 2013, **9**, 98-106.
 20. J. M. Oh, S. J. Choi, G. E. Lee, S. H. Han and J. H. Choy, *Adv. Funct. Mater.*, 2009, **19**, 1617-1624.
 21. L. O. Torres-Dorante, J. Lammel, H. Kuhlmann, T. Witzke and H. W. Olf, *J. Plant Nutr. Soil Sci.-Z. Pflanzenernahr. Bodenkd.*, 2008, **171**, 777-784.
 22. Z. P. Xu, Q. H. Zeng, G. Q. Lu and A. B. Yu, *Chem. Eng. Sci.*, 2006, **61**, 1027-1040.
 23. C. Mousty, *Appl. Clay Sci.*, 2004, **27**, 159-177.

24. K. H. Goh, T. T. Lim and Z. Dong, *Water Res.*, 2008, **42**, 1343-1368.
25. B. F. Sels, D. E. De Vos and P. A. Jacobs, *Catal. Rev.-Sci. Eng.*, 2001, **43**, 443-488.
26. T. Stimpfling and F. Leroux, *Chem. Mat.*, 2010, **22**, 974-987.
27. Z. Gu, A. C. Thomas, Z. P. Xu, J. H. Campbell and G. Q. Lu, *Chem. Mat.*, 2008, **20**, 3715-3722.
28. Z. Gu, A. Wu, L. Li and Z. P. Xu, *Pharmaceutics*, 2014, **6**, 235-248.
29. Y. F. Xu, Y. C. Dai, J. Z. Zhou, Z. P. Xu, G. R. Qian and G. Q. M. Lu, *J. Mater. Chem.*, 2010, **20**, 4684-4691.
30. Z. Y. Lu, W. Zhu, X. D. Lei, G. R. Williams, D. O'Hare, Z. Chang, X. M. Sun and X. Duan, *Nanoscale*, 2012, **4**, 3640-3643.
31. M. Adachi-Pagano, C. Forano and J. P. Besse, *Chem. Commun.*, 2000, 91-92.
32. S. O'Leary, D. O'Hare and G. Seeley, *Chem. Commun.*, 2002, 1506-1507.
33. T. Hibino and W. Jones, *J. Mater. Chem.*, 2001, **11**, 1321-1323.
34. G. Hu, N. Wang, D. O'Hare and J. J. Davis, *J. Mater. Chem.*, 2007, **17**, 2257-2266.
35. G. Hu, N. Wang, D. O'Hare and J. Davis, *Chem. Commun.*, 2006, 287-289.
36. W. R. Zhao, J. L. Gu, L. X. Zhang, H. R. Chen and J. L. Shi, *J. Am. Chem. Soc.*, 2005, **127**, 8916-8917.
37. F. Wypych, G. A. Bubniak, M. Halma and S. Nakagaki, *J. Colloid Interface Sci.*, 2003, **264**, 203-207.
38. Y. Wang, W. S. Yang and J. J. Yang, *Electrochem. Solid State Lett.*, 2007, **10**, A233-A236.
39. H. Zhang, D. K. Pan and X. Duan, *J. Phys. Chem. C*, 2009, **113**, 12140-12148.
40. H. Zhang, K. Zou, H. Sun and X. Duan, *J. Solid State Chem.*, 2005, **178**, 3485-3493.
41. C. P. Chen, L. K. Yee, H. Gong, Y. Zhang and R. Xu, *Nanoscale*, 2013, **5**, 4314-4320.
42. D. K. Pan, H. Zhang, T. Fan, J. G. Chen and X. Duan, *Chem. Commun.*, 2011, **47**, 908-910.
43. Y. Zhao, S. He, M. Wei, D. G. Evans and X. Duan, *Chem. Commun.*, 2010, **46**, 3031-3033.
44. M. F. Shao, F. Y. Ning, Y. F. Zhao, J. W. Zhao, M. Wei, D. G. Evans and X. Duan, *Chem. Mat.*, 2012, **24**, 1192-1197.
45. M. F. Shao, F. Y. Ning, J. W. Zhao, M. Wei, D. G. Evans and X. Duan, *J. Am. Chem. Soc.*, 2012, **134**, 1071-1077.
46. J. Wang, R. R. Zhu, B. Gao, B. Wu, K. Li, X. Y. Sun, H. Liu and S. L. Wang, *Biomaterials*, 2014, **35**, 466-478.
47. X. F. Zhang, J. Wang, R. M. Li, Q. H. Dai, R. Gao, Q. Liu and M. L. Zhang, *Ind. Eng. Chem. Res.*, 2013, **52**, 10152-10159.
48. A. N. Ay, D. Konuk and B. Zumreoglu-Karan, *Mater. Sci. Eng. C-Mater. Biol. Appl.*, 2011, **31**, 851-857.
49. D. A. Li, Y. T. Zhang, M. Yu, J. Guo, D. Chaudhary and C. C. Wang, *Biomaterials*, 2013, **34**, 7913-7922.
50. D. H. Park, J. E. Kim, J. M. Oh, Y. G. Shul and J. H. Choy, *J. Am. Chem. Soc.*, 2010, **132**, 16735-16736.
51. L. Li, R. Z. Ma, N. Iyi, Y. Ebina, K. Takada and T. Sasaki, *Chem. Commun.*, 2006, 3125-3127.
52. R. Z. Ma and T. Sasaki, *Adv. Mater.*, 2010, **22**, 5082-5104.
53. L. Li, Y. J. Feng, Y. S. Li, W. R. Zhao and J. L. Shi, *Angew. Chem.-Int. Edit.*, 2009, **48**, 5888-5892.
54. L. Huang, D. C. Chen, Y. Ding, S. Feng, Z. L. Wang and M. L. Liu, *Nano Lett.*, 2013, **13**, 3135-3139.
55. X. T. Chen, F. Mi, H. Zhang and H. Q. Zhang, *Mater. Lett.*, 2012, **69**, 48-51.
56. H. Zhang, R. Qi, D. G. Evans and X. Duan, *J. Solid State Chem.*, 2004, **177**, 772-780.
57. Z. Gu, B. E. Rolfe, A. C. Thomas and Z. P. Xu, *Curr. Pharm. Design*, 2013, **19**, 6330-6339.
58. A. N. Ay, B. Zumreoglu-Karan, A. Temel and V. Rives, *Inorg. Chem.*, 2009, **48**, 8871-8877.
59. S. Mornet, S. Vasseur, F. Grasset and E. Duguet, *J. Mater. Chem.*, 2004, **14**, 2161-2175.
60. A. K. Gupta and M. Gupta, *Biomaterials*, 2005, **26**, 3995-4021.
61. K. Shang, J. Y. Zhu, X. M. Meng, Z. Q. Cheng and S. Y. Ai, *Biosens. Bioelectron.*, 2012, **37**, 107-111.
62. S. K. Khetan and T. J. Collins, *Chem. Rev.*, 2007, **107**, 2319-2364.
63. D. K. Pan and H. Zhang, *Acta Chim. Sin.*, 2011, **69**, 1545-1552.
64. C. M. Dai, S. U. Geissen, Y. L. Zhang, Y. J. Zhang and X. F. Zhou, *Environ. Pollut.*, 2011, **159**, 1660-1666.
65. Z. P. Xu, R. Xu and H. C. Zeng, *Nano Lett.*, 2001, **1**, 703-706.
66. Z. Hasan, J. Jeon and S. H. Jung, *J. Hazard. Mater.*, 2012, **209**, 151-157.
67. X. M. Liu, Z. D. Huang, S. W. Oh, B. Zhang, P. C. Ma, M. M. F. Yuen and J. K. Kim, *Compos. Sci. Technol.*, 2012, **72**, 121-144.
68. H. Li, Z. X. Wang, L. Q. Chen and X. J. Huang, *Adv. Mater.*, 2009, **21**, 4593-4607.
69. M. C. Orilall and U. Wiesner, *Chem. Soc. Rev.*, 2011, **40**, 520-535.
70. N. T. H. Trang, H. V. Ngoc, N. Lingappan and D. J. Kang, *Nanoscale*, 2014, **6**, 2434-2439.
71. B. Wang, G. R. Williams, Z. Chang, M. Jiang, J. Liu, X. Lei and X. Sun, *ACS Appl. Mater. Interfaces*, 2014, **6**, 16304-16311.
72. Y. H. Gu, Z. Y. Lu, Z. Chang, J. F. Liu, X. D. Lei, Y. P. Li and X. M. Sun, *J. Mater. Chem. A*, 2013, **1**, 10655-10661.
73. Z. Y. Lu, Z. Chang, W. Zhu and X. M. Sun, *Chem. Commun.*, 2011, **47**, 9651-9653.
74. W. Zhu, Z. Y. Lu, G. X. Zhang, X. D. Lei, Z. Chang, J. F. Liu and X. M. Sun, *J. Mater. Chem. A*, 2013, **1**, 8327-8331.
75. Z. Tang, C. H. Tang and H. Gong, *Adv. Funct. Mater.*, 2012, **22**, 1272-1278.
76. C. Guan, X. L. Li, Z. L. Wang, X. H. Cao, C. Soci, H. Zhang and H. J. Fan, *Adv. Mater.*, 2012, **24**, 4186-4190.
77. H. F. Bao, J. P. Yang, Y. Huang, Z. P. Xu, N. Hao, Z. X. Wu, G. Q. Lu and D. Y. Zhao, *Nanoscale*, 2011, **3**, 4069-4073.
78. J. Liu, R. Harrison, J. Z. Zhou, T. T. Liu, C. Z. Yu, G. Q. Lu, S. Z. Qiao and Z. P. Xu, *J. Mater. Chem.*, 2011, **21**, 10641-10644.
79. J. H. Yang, S. Y. Lee, Y. S. Han, K. C. Park and J. H. Choy, *Bull. Korean Chem. Soc.*, 2003, **24**, 499-503.
80. S. H. Hwang, S. C. Jung, S. M. Yoon and D. K. Kim, *J. Phys. Chem. Solids*, 2008, **69**, 1061-1065.
81. L. J. Wang, J. L. Shi, Y. Zhu, Q. J. He, H. Y. Xing, J. Zhou, F. Chen and Y. Chen, *Langmuir*, 2012, **28**, 4920-4925.
82. Z. An, S. Lu, J. He and Y. Wang, *Langmuir*, 2009, **25**, 10704-10710.
83. X. G. Kong, X. Y. Rao, J. B. Han, M. Wei and X. Duan, *Biosens. Bioelectron.*, 2010, **26**, 549-554.
84. F. Bellezza, A. Alberani, T. Posati, L. Tarpani, L. Latterini and A. Cipiciani, *J. Inorg. Biochem.*, 2012, **106**, 134-142.

85. F. Bellezza, A. Cipiciani, L. Latterini, T. Posati and P. Sassi, *Langmuir*, 2009, **25**, 10918-10924.
86. S. Yan, B. E. Rolfe, B. Zhang, Y. H. Mohammed, W. Gu and Z. P. Xu, *Biomaterials*, 2014, **35**, 9508-9516.
87. Z. Gu, H. Zuo, A. Wu and Z. P. Xu, 3rd Symposium on Innovative Polymers for Controlled Delivery, Suzhou, China, 2014, accepted.
88. B. X. Li, J. He, D. G. Evans and X. Duan, *Int. J. Pharm.*, 2004, **287**, 89-95.
89. J. U. Ha and M. Xanthos, *Appl. Clay Sci.*, 2010, **47**, 303-310.
90. D. X. Li, X. J. Xu, J. Xu and W. G. Hou, *Colloid Surf. A-Physicochem. Eng. Asp.*, 2011, **384**, 585-591.
91. X. J. Guo, L. H. Zhao, L. Zhang and J. Li, *Appl. Surf. Sci.*, 2012, **258**, 2404-2409.
92. H. Hu, X. B. Wang, S. L. Xu, W. T. Yang, F. J. Xu, J. Shen and C. Mao, *J. Mater. Chem.*, 2012, **22**, 15362-15369.
93. H. Hu, K. M. Xiu, S. L. Xu, W. T. Yang and F. J. Xu, *Bioconjugate Chem.*, 2013, **24**, 968-978.
94. P. R. Wei, S. H. Cheng, W. N. Liao, K. C. Kao, C. F. Weng and C. H. Lee, *J. Mater. Chem.*, 2012, **22**, 5503-5513.
95. K. Matyjaszewski and J. H. Xia, *Chem. Rev.*, 2001, **101**, 2921-2990.
96. N. Singh, J. Wang, M. Ulbricht, S. R. Wickramasinghe and S. M. Husson, *J. Memb. Sci.*, 2008, **309**, 64-72.
97. L. E. van Vlerken, T. K. Vyas and M. M. Amiji, *Pharm. Res.*, 2007, **24**, 1405-1414.
98. D. E. Owens and N. A. Peppas, *Int. J. Pharm.*, 2006, **307**, 93-102.
99. H. Otsuka, Y. Nagasaki and K. Kataoka, *Adv. Drug Deliv. Rev.*, 2003, **55**, 403-419.
100. L. N. M. Ribeiro, A. C. S. Alcantara, M. Darder, P. Aranda, F. M. Araujo-Moreira and E. Ruiz-Hitzky, *Int. J. Pharm.*, 2014, **463**, 1-9.
101. V. Ambroggi, L. Perioli, M. Ricci, L. Pulcini, M. Nocchetti, S. Giovagnoli and C. Rossi, *Microporous Mesoporous Mat.*, 2008, **115**, 405-415.
102. M. del Arco, A. Fernandez, C. Martin and V. Rives, *J. Solid State Chem.*, 2010, **183**, 3002-3009.
103. V. Rives, M. del Arco and C. Martin, *J. Control. Release*, 2013, **169**, 28-39.
104. B. Wang, H. Zhang, D. G. Evans and X. Duan, *Mater. Chem. Phys.*, 2005, **92**, 190-196.
105. M. R. Islam, Z. H. Guo, D. Rutman and T. J. Benson, *RSC Adv.*, 2013, **3**, 24247-24255.
106. J. F. Lu, K. Minami, S. Takami and T. Adschiri, *Chem. Eng. Sci.*, 2013, **85**, 50-54.
107. D. P. Qiu, Y. H. Li, X. Y. Fu, Z. Jiang, X. Y. Zhao, T. Wang and W. G. Hou, *Chin. J. Chem.*, 2009, **27**, 445-451.
108. J. Q. Jiang, Y. W. Zhang, Y. H. Zheng and P. K. Jiang, *Chem. Eng. Technol.*, 2013, **36**, 1371-1377.
109. A. E. Nel, L. Madler, D. Velegol, T. Xia, E. M. V. Hoek, P. Somasundaran, F. Klaessig, V. Castranova and M. Thompson, *Nat. Mater.*, 2009, **8**, 543-557.
110. J. C. Sun, J. J. Li, H. Fan and S. Y. Ai, *J. Mat. Chem. B*, 2013, **1**, 5436-5442.
111. L. Li, W. Gu, J. Liu, S. Yan and Z. P. Xu, *Nano Research*, 2014. DOI 10.1007/s12274-014-0552-6.
112. S. Cho, S. C. Hong and S. Kim, *J. Mater. Chem. C*, 2014, **2**, 450-457.
113. S. Cho, S. Jung, S. Jeong, J. Bang, J. Park, Y. Park and S. Kim, *Langmuir*, 2013, **29**, 441-447.
114. J. L. Vivero-Escoto, Slowing, II, B. G. Trewyn and V. S. Y. Lin, *Small*, 2010, **6**, 1952-1967.
115. M. J. Alonso, *Biomed. Pharmacother.*, 2004, **58**, 168-172.
116. P. Couvreur and C. Vauthier, *Pharm. Res.*, 2006, **23**, 1417-1450.
117. D. Peer, J. M. Karp, S. Hong, O. C. FaroKhazad, R. Margalit and R. Langer, *Nat. Nanotechnol.*, 2007, **2**, 751-760.
118. E. O. Hanrahan, A. M. Gonzalez-Angulo, S. H. Giordano, R. Rouzier, K. R. Broglio, G. N. Hortobagyi and V. Valero, *J. Clin. Oncol.*, 2007, **25**, 4952-4960.
119. Z. Y. Xia, N. Du, J. Q. Liu and W. G. Hou, *Chem. J. Chin. Univ.-Chin.*, 2013, **34**, 596-600.
120. L. Yan, W. Chen, X. Y. Zhu, L. B. Huang, Z. G. Wang, G. Y. Zhu, V. A. L. Roy, K. N. Yu and X. F. Chen, *Chem. Commun.*, 2013, **49**, 10938-10940.
121. Z. Gu, B. E. Rolfe, Z. P. Xu, J. H. Campbell, G. Q. Lu and A. C. Thomas, *Adv. Healthc. Mater.*, 2012, **1**, 669-673.
122. D. J. Bharali, D. W. Lucey, H. Jayakumar, H. E. Pudavar and P. N. Prasad, *J. Am. Chem. Soc.*, 2005, **127**, 11364-11371.
123. C. P. Leamon and P. S. Low, *Drug Discov. Today*, 2001, **6**, 44-51.
124. P. S. Low, W. A. Henne and D. D. Doorneweerd, *Acc. Chem. Res.*, 2008, **41**, 120-129.
125. J. A. Reddy, V. M. Allagadda and C. P. Leamon, *Curr. Pharm. Biotechnol.*, 2005, **6**, 131-150.
126. A. M. Bashi, S. M. Haddawi and M. A. Mezaal, *Arab. J. Sci. Eng.*, 2013, **38**, 1663-1680.
127. J. H. Choy, J. S. Jung, J. M. Oh, M. Park, J. Jeong, Y. K. Kang and O. J. Han, *Biomaterials*, 2004, **25**, 3059-3064.
128. L. L. Qin, S. L. Wang, R. Zhang, R. R. Zhu, X. Y. Sun and S. D. Yao, *J. Phys. Chem. Solids*, 2008, **69**, 2779-2784.
129. A. C. Thomas and J. H. Campbell, *Thromb. Res.*, 2003, **109**, 65-69.
130. A. C. Thomas and J. H. Campbell, *Atherosclerosis*, 2004, **176**, 73-81.
131. A. C. Thomas and J. H. Campbell, *J. Control. Release*, 2004, **100**, 357-377.